Available online at www.sciencedirect.com
SCIENCE DIRECT®
Journal of Sound and Vibration 287 (2005) 45–75
JOURNAL OF SOUND AND VIBRATION
www.elsevier.com/locate/jsvi

Sound transmission into an axisymmetric enclosure

D. Brenot*

EDF R & D, Analysis in Mechanics and Acoustic Department, Avenue du Général de Gaulle, BP 408, 92 141 Clamart Cedex, France

Received 10 October 2003; received in revised form 24 September 2004; accepted 25 October 2004
Available online 16 February 2005

Abstract

A method to compute the power spectral density of sound transmitted on the axis of an axisymmetric enclosure for a wide frequency band is presented. This method is very easy to program.

Even when the driving excitation is not axisymmetric, the method only requires the in vacuo structural modes to be calculated. This can be achieved by a finite element calculation, since the density of these modes tends to zero while the frequency tends to infinity.

The results improve as the frequency increases, but generally they are already valid at the first resonance of the elastic shell.

The problem comprises three coupled domains: external acoustics, internal acoustics, and structural vibrations. The internal acoustics is formulated with acoustic dissipation, modelled by locally reacting wall impedance superimposed onto the motion of the elastic structure.

It can be solved through three original arguments:

- The joint use of an integral representation and a modal decomposition of the Helmholtz equation results in an integral relation between the pressure inside the cavity, the wall acceleration and the acoustic and structure damping.
- This integral expression can be developed with the stationary phase method since the axisymmetric modes of most aeronautical structures are acoustically fast, even below the coincidence frequency, and only these modes are needed to compute the pressure on the axis. As a result, the structure zones which contribute to the pressure on a specific point of the axis are very localized. Generally, there is only one zone: the parallel constituted by the points nearest to this axis point.

*201 Avenue du Bois de Verrières, Antony 92 160, France. Tel./fax: +33 1 47 653978.
E-mail address: dobrenot@wanadoo.fr (D. Brenot).

0022-460X/$ - see front matter
doi:10.1016/j.jsv.2004.10.048

- A wall pressure jump formulation provides a second equation for the pressure on the axis point; the equality of both pressure expressions leads to a local relation between the pressure jump expression and the wall acceleration: the fluid–structure coupling for axisymmetric modes is quite local.

Once the modal coupling terms are known, the wall acceleration, and therefore the internal pressure on the axis, can be computed by using only the structural modes.

1. Literature review

Initially limited to the transmission of airborne noise into an aircraft fuselage, noise transmission-related problems have received significant attention, particularly since noise levels in modern launchers exceed acceptable safety criteria payloads.

The most advanced noise transmission analyses were briefly reviewed by Dowell [1] with respect to all flight vehicles.

Smith [2] was among the first authors to model a fuselage with an infinite cylinder, for which an analytical expression can be written.

To some extent, Koval [3–11] extended Smith's results to finite shells. He systematically introduced panel curvature, internal pressurization, cavity resonance, stiffeners and orthotropic panels into his analysis.

Cockburn and Jolly [12] considered the structural and acoustic modes of a stiffened cylindrical shell and enclosed volume.

Pope [13–18] studied the acoustic band-limited power flow into an enclosure. He needed two main simplifying assumptions: the first one was that the coupling between the structural and acoustic modes was weak, which, however, in no way excludes well-coupled modes which occur when acoustic and structural modes have resonance frequencies that are closely spaced relative to the modal bandwidths. But Unruh [19], using a finite element calculation, showed that this assumption had to be treated with caution: at low frequencies, there could be a strong coupling between structural and cavity modes. The second assumption was that the structural inter-modal coupling could be neglected, for which the preceding remark was also true.

Lyon [20] applied the Statistical Energy Analysis (SEA) method to structures with complex shapes, assuming that it was unnecessary to know with accuracy the frequencies of the modes, provided that they were sufficiently numerous.

The authors have generally modelled the structure either as a cylinder, like Koval [3,4,7–10] and Smith [2], or as an assembly of panels like Vaicatis [21–23] and Koval [11], with simply supported or clamped boundary conditions. These panels can be flat and rectangular [21–23] or curved [11].

Chang and Vaicatis [24] studied a semi-cylindrical enclosure closed by a floor and two rigid walls. The individual panels could be formed into linear arrays joined up by stiffeners. Vaicatis [21] used the transfer matrix method of Lin [25,26] to solve the equations associated with these discrete elements. Pope, Wilby, Willis and Hayes [13,14,17,18] proposed a complete analytical model of a propeller aircraft by means of a cylinder with a floor.

All these authors presented a modal approach to the problem.

In general, the internal pressure was expressed as a function of the displacement of the structure via the Green function of the interior problem.

The external pressure was the sum of the pressure on the blocked structure and the acoustic field radiated by the structure. The latter was related to the displacement of the structure via the Green function of the exterior problem.

These integral expressions were coupled by the equations of the motion of the structure, the excitation of which was the difference between the external and internal wall pressures.

A system of algebraic equations was thus formed to obtain the modal response of the transmitting structure.

The final result was achieved through the concept of acoustic power flow balance: the net time-averaged power flow into the receiving volume equalled the net time-averaged acoustic power dissipated on the internal wall, defined via a mean absorption coefficient on its surface.

Particular attention must be paid to the formulation of Dowell, Gorman and Smith [27], which provides a clear understanding of the coupling between the elastic structure and the cavity: to express the motion of the structure, they used the basis of the in vacuo modal shapes of the structure, and to express the Green function of the cavity, they used the rigid-wall eigenmodes of the cavity.

They showed that the nature of the coupling between the structure and cavity was gyroscopic and thus that the structure without damping and internal non-dissipative fluid constituted a system without damping. A numerical method for computing the modes of this coupled system was developed by Meirovitch [28]. He modelled the fluid damping with locally reactive wall impedance and showed which coupling this wall impedance introduced between the cavity modes.

2. Proposed method

Our starting point will also be a formal development of the internal pressure on a modal basis as used by Dowell [27]. We will then develop three original basic arguments to perform the complete calculation.

The first argument is that the modal expansion will be combined with an integral formulation using the Green function in an undefined domain. We will show that an integral equation can be obtained linking the pressure inside the cavity, the wall acceleration and the acoustic and structural damping, the importance of which will be discussed in the formulation and resolution of the problem.

Then we will show that the pressure along the axis of an axisymmetric enclosure depends only on the axisymmetric modes, even when the driving excitation is not axisymmetric. For most aeronautical airborne structures, these modes are acoustically fast. Therefore, their spatial variations are smooth in comparison with the phase of the Green function and the method of the stationary phase can be applied to the integral expression derived from the first argument. This leads to the second basic argument stating that the zones of the structure which contribute to the noise at one point of the axis are localized on the shell. These zones correspond to the Green

function stationary phases. Generally there is only one zone: the parallel constituting the points nearest to this axis point.

The stationary phase method will also be used to establish the third argument, i.e. that the coupling between the fluid and the axisymmetric modes of the structure may be considered as local. To obtain this result, another equation for the pressure will be given as an integral expression containing the wall-pressure jump. The stationary phase method will be used to derive a local relation between the wall-pressure jump and the wall acceleration for each localized zone mentioned in the second argument.

Finally, because the first argument links the internal pressure on the axis to the wall acceleration and the second one provides the wall jump pressure term to be introduced in the wall acceleration equation, the proposed method results in a calculation limited to the structure. The numerical resolution of the Helmholtz equation, which would be intractable because of the high modal density of the cavity, is thus avoided.

By contrast, the remaining computation of the axisymmetric modes of the structure can easily be calculated with the finite element method, since their density tends to zero as the frequency tends to infinity.

This method gives the spectral power density of the pressure along the axis of an axisymmetric enclosure for any external driving excitation, on a wide frequency band.

It can be applied at high frequencies for any structure, and at any frequency for most aeronautical airborne structures. An easy graphic process can be used to verify its applicability when subject to caution at low frequency.

An experiment that shows the relevance of this calculation is presented in chapter 8.

3. Complete formulation of the problem

Let the cavity occupy a volume V and be surrounded by a flexible wall surface S, and two reflecting rigid ends F_1 and F_2. For the sake of simplicity, the thickness of the wall will be assumed to be null.

Fig. 1 represents the half meridian of an axisymmetric structure and contains all the equations that will be used hereafter Eqs. (9)–(11).

Let the displacement u of the flexible surface satisfy a shell equation:

$$-\omega^2 Mu + Ku = -e + n(p^i - p^e)\big|_S, \quad \text{Boundary conditions on } S \cap (F_1 \cup F_2), \tag{1}$$

where M is the symmetric mass operator, K the symmetric stiffness operator and n the outward normal vector.

The boundary conditions have to be determined only at the intersection of S and the ends F_1, F_2.

The external driving of the structure is the known data e, which need not be axisymmetric. It is a wall motion-independent driving as, for instance, the blocked structure acoustic pressure (rocket motor noise, fan noise, etc.), a boundary layer or an applied force field. But the displacement u of the shell itself induces an internal pressure p^i and an external pressure p^e. The shell reacts to the difference between these two pressures on the wall: $n(p^i - p^e)\big|_S$ is simply the fluid–structure coupling term.

The component of the internal pressure at the angular frequency ω satisfies the familiar Helmholtz equation and the associated boundary conditions:

$$\begin{aligned} &\Delta p^i + k^2 p^i = 0 \quad \text{in } V, \\ &\left.\frac{\partial p^i}{\partial n}\right|_S = \rho\omega^2(u,n), \\ &\left.\frac{\partial p^i}{\partial n}\right|_{F_1 \cup F_2} = 0. \end{aligned} \tag{2}$$

An analogous Helmholtz equation is assumed to express the external pressure in the exterior domain $\overline{V}$:

$$\begin{aligned} &\Delta p^e + k^2 p^e = 0 \text{ in } \overline{V}, \\ &\left.\frac{\partial p^e}{\partial n}\right|_S = \rho\omega^2(u,n), \\ &\left.\frac{\partial p^e}{\partial n}\right|_{F_1 \cup F_2} = 0, \quad \text{Sommerfeld condition.} \end{aligned} \tag{3}$$

In these equations, ρ is the equilibrium fluid density and $k = \omega/c$ is the acoustic wave number, c being the acoustic velocity.

Eqs. (1)–(3) do not take into account the damping terms. Indeed, both the structure and the fluid dissipate energy.

No simple description, if any at all, is available for the structural damping. Most of the energy dissipated in shells is lost into the end supports and thus greatly depends on the means of support and the structures the shell is attached to. Nevertheless, a simple way to consider the in vacuo structural damping is to assume for the dissipation operator the following form:

$$-2\mathrm{i}\omega\varepsilon u, \tag{4}$$

ε being diagonal in the in vacuo modal basis of the shell.

When the modes are sufficiently spaced in frequency, their loss coefficient can be measured as the logarithmic decrement of the root mean square value of the wall acceleration after any excitation at the associated frequency has been stopped. It is also a way to verify that ε is diagonal (in fact, the acoustic energy loss is included in this process and the experiment should be performed in vacuo to conform to the equations of Fig. 1).

The fluid possesses an inherent viscosity, the effect of which appears at very high frequency and may almost always be neglected in the problem under consideration.

By contrast, the wall itself dissipates part of the sound especially when it is covered with a sound-absorbing coating. Its absorbing power can be measured with an impedance tube, and is characterized by a locally reactive impedance, which may be complex; only its real part implies dissipation.

This impedance is quite different from the wall impedance relative to its elastic behaviour, which is not locally reactive: the motion of one point of the wall depends on the pressure on the whole shell and not only on the local pressure.

Pierce [29] has shown that this acoustic impedance was equivalent to the Sabine absorption coefficient used to compute the reverberation time in a cavity with an infinitely rigid wall.

Furthermore, both the impedance ρc_L and the thickness of the material constituting the structure contribute to this wall impedance. Indeed, the latter includes acoustic leakage to the exterior resulting from the variations in acceleration inside the thickness of the shell, not considered in the shell equations (the velocities on the neutral surface and on the boundary inside which the Helmholtz equation is applicable are assumed to be the same).

This locally reactive impedance may, in addition, include the possible presence of the acoustic boundary layer, thereby avoiding use of the Navier–Stokes equations in the neighbourhood of the wall.

In any event, the dissipation of sound energy takes place in the neighbourhood of the wall.

To put it simply, it is sufficient to say that the Helmholtz equation does not apply entirely to the volume V enclosed by the neutral surface of the shell S and the ends F_1, F_2, but to a volume V', slightly smaller and enclosed by a boundary S'.

The surface S' will transmit the normal acceleration of the surface S. In addition, it will introduce a normal velocity difference $\left(\left(\partial u^{s'}/\partial t\right) - \left(\partial u^{s}/\partial t\right)\right), n\big)$ assumed to be related to the wall pressure through a locally reactive impedance $Z_{S'}$, eventually complex and depending upon the frequency:

$$p^i(t) = Z_{S'}\left(\left(\frac{\partial u^{S'}}{\partial t} - \frac{\partial u^{s}}{\partial t}\right), n\right). \tag{5}$$

The acceleration normal to the surface $S^{'}$ will therefore be

$$\left(\frac{\partial^2 u^{s'}(t)}{\partial t^2}, n\right) = \left(\frac{\partial^2 u^{s}(t)}{\partial t^2}, n\right) + \left(\frac{\partial p^i(t)/\partial t}{Z_{S'}}\right). \tag{6}$$

It is on this surface $S^{'}$ that the boundary condition of (2) (normal derivative of the pressure) should be imposed.

Retaining the same notation for a function and its Fourier transform, we will write the boundary condition on S instead of S', since S is sufficiently close to S':

$$\left.\frac{\partial p^i}{\partial n}(\omega)\right|_S = \rho\omega^2(u, n) + \frac{\mathrm{i}k}{\zeta}p^i(\omega), \tag{7}$$

and we will suppose that the Helmholtz equation applies throughout the whole volume V. By definition, $\zeta(\omega) = Z_S(\omega)/\rho c$ is the normalized acoustic impedance.

The same could be applied to the external problem, the equations of which would be

$$\begin{aligned}
&\Delta p^e + k^2 p^e = 0 \quad \text{in } \overline{V},\\
&\left.\frac{\partial p^e}{\partial n}\right|_S = \rho\omega^2(u, n) - \mathrm{i}\frac{k}{\zeta}p^e,\\
&\left.\frac{\partial p^e}{\partial n}\right|_{F_1 \cup F_2} = 0, \quad \text{Sommerfeld condition.}
\end{aligned} \tag{8}$$

But for the external problem the dissipation due to the acoustic energy radiated in the far field is predominant. Therefore, this complication is not worthwhile.

The final complete set of equations is as follows:

$$\begin{aligned}
&\Delta p^i + k^2 p^i = 0 \quad \text{in } V,\\
&\left(\frac{\partial p^i}{\partial n} - \frac{\mathrm{i}k}{\zeta} p^i\right)\Big|_S = \rho\omega^2(u,n),\\
&\left.\frac{\partial p^i}{\partial n}\right|_{F_1 \cup F_2} = 0,
\end{aligned} \tag{9}$$

$$-\omega^2 Mu - 2\mathrm{i}\omega\varepsilon u + Ku = -e + n(p^i - p^e)\big|_S \quad \text{on } S, \quad \text{Boundary conditions on } S \cap (F_1 \cup F_2), \tag{10}$$

$$\begin{aligned}
&\Delta p^e + k^2 p^e = 0 \quad \text{in } \overline{V},\\
&\left.\frac{\partial p^e}{\partial n}\right|_S = \rho\omega^2(u,n),\\
&\left.\frac{\partial p^e}{\partial n}\right|_{F_1 \cup F_2} = 0, \quad \text{Sommerfeld condition.}
\end{aligned} \tag{11}$$

Obviously, in order to neglect sound dissipation at the wall or structure damping, it is sufficient to give very large values to ζ or very small values to ε.

Using the results of Refs. [27,28], it is demonstrated in Ref. [30a] that the complete problem defined in Fig. 1 still has a unique finite solution.

More precisely, the system consisting of Eqs. (1) and (2) (internal fluid and elastic structure) is not damped in the absence of mechanical or acoustic dissipation. Thus, there are coupled fluid–structural modes, and at their frequencies, the response of the system could theoretically be infinite valued.

Eq. (3) (external fluid) introduces a natural damping by acoustic radiation owing to the energy loss in the far field. The response of the coupled fluid–structural modes becomes finite, but the levels inside the cavity may be irrelevantly high.

In other terms, Eqs. (1) and (2) remain singular for the eigenvalues corresponding to the nullity of their right sides (in vacuo modes for Eq. (1) and rigid wall modes for Eq. (2)). At these eigenfrequencies, the number and frequency density of which tend to infinity with the frequency, orthogonality relations have to be written instead of Eqs. (1) and (2).

By contrast, Eqs. (9)–(11) have a unique solution whatever their right sides may be. In addition, the associated equations are physically relevant since both mechanical and acoustic dissipations are considered.

Moreover, it will be demonstrated that the acoustic wall impedance and the structural damping are fundamental parameters for determining the pressure level inside the cavity.

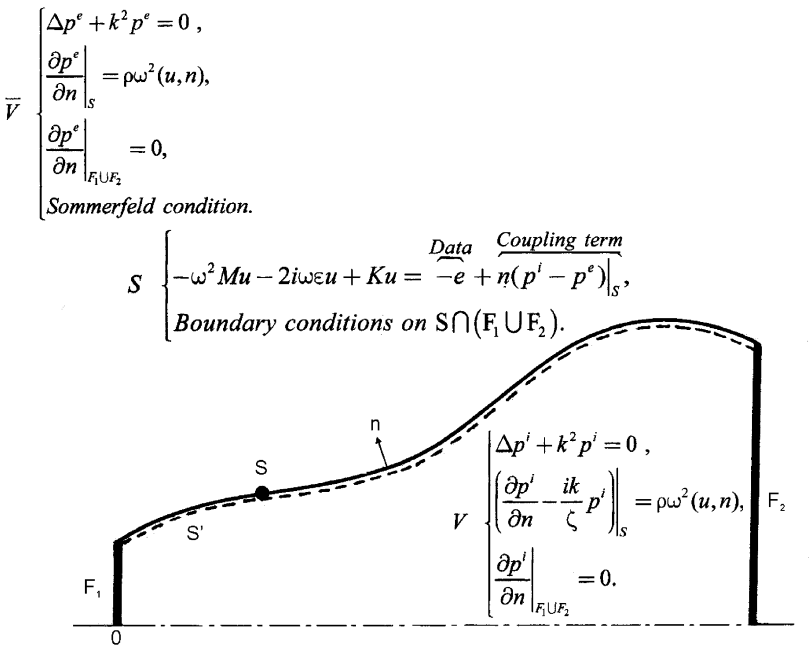

Fig. 1. The problem to be solved.

4. Solution of the acoustic interior problem

4.1. Green formulation and modal expansion (first argument)

Let u_n be the Neumann modes of the cavity (rigid wall modes):

$$\Delta u_n + \gamma_n^2 u_n = 0,$$
$$\left.\frac{\partial u_n}{\partial n}\right|_{S \cup F_1 \cup F_2} = 0. \tag{12}$$

The eigenvalues $-\gamma_n^2$ are real and the set u_n constitutes an orthonormal basis in the space of solutions for the problem (9) (namely the Sobolev space $H^1(V)$), even when the boundary condition is not a rigid wall.

The Green function G^ζ associated with the problem (9):

$$\Delta G^\zeta + k^2 G^\zeta = -\delta(x-y) \quad \text{in } V,$$
$$\left.\left(\frac{\partial G^\zeta}{\partial n} - \frac{ik}{\zeta} G^\zeta\right)\right|_{S \cup F_1 \cup F_2} = 0, \tag{13}$$

(where ζ is infinite valued on $F_1 \cup F_2$ in accordance with the boundary conditions in Eq. (9)) can be expanded in the biorthogonal set of eigenvectors w_n and v_n of the homogeneous problem

associated with (13) and its adjoint problem [31]:

$$G^{\zeta}(x,y)=\sum_{n=-\infty}^{n=+\infty}\frac{w_n(x)\overline{v}_n(y)}{k_n^2-k^2}=\sum_{n=-\infty}^{n=+\infty}\frac{w_n(x)w_n(y)}{k_n^2-k^2}, \tag{14}$$

where a bar over a symbol means, here and hereafter, the conjugated value of a complex-valued parameter and:

$$\begin{aligned}&\Delta w_n+k_n^2 w_n=0,\\&\left(\frac{\partial w_n}{\partial n}-\frac{\mathrm{i}k}{\zeta}w_n\right)\Big|_{S\cup F_1\cup F_2}=0,\end{aligned} \tag{15}$$

$$\begin{aligned}&\Delta v_n+\overline{k}_n^2 v_n=0,\\&\left(\frac{\partial v_n}{\partial n}+\frac{\mathrm{i}k}{\overline{\zeta}}v_n\right)\Big|_{S\cup F_1\cup F_2}=0.\end{aligned} \tag{16}$$

Therefore, the internal pressure can be written as

$$\begin{aligned}p^i(x,k,\zeta,\varepsilon)&=\int_S G^{\zeta}(x,y)\rho\omega^2(u(y,k,\varepsilon),n_y)\,\mathrm{dS}(y)\\&=\sum_{n=-\infty}^{n=+\infty}\frac{\int_S\rho\omega^2(u(y,k,\varepsilon),n_y)w_n(y)\,\mathrm{dS}(y)}{k_n^2-k^2}w_n(x)=\sum_{n=-\infty}^{n=+\infty}\alpha_n(k,\zeta,\varepsilon)w_n(x)\end{aligned} \tag{17}$$

in which every mode $w_n(x)$ can be expressed as

$$w_n(x)=\sum_{p=-\infty}^{p=+\infty}\left(\int_V w_n\overline{u_p}\,\mathrm{d}v\right)u_p(x). \tag{18}$$

The eigenvalues of Eq. (15), $-k_n^2$, counted with their multiplicity order, tend towards $-\gamma_n^2$ when $1/|\zeta|\to 0$, and are complex. A simple application of the Green formula in Eqs. (12) and (15):

$$(k_n^2-\gamma_p^2)\int_V w_n\overline{u_p}\,\mathrm{d}v+\mathrm{i}k\int_S\frac{w_n\overline{u_p}}{\zeta}\,\mathrm{d}S=0, \tag{19}$$

shows that

$$\lim_{\substack{|\zeta|\to\infty\\ k_n^2\to\gamma_n^2\neq\gamma_p^2}}\int_V w_n\overline{u_p}\,\mathrm{d}v=\frac{-\mathrm{i}k}{k_n^2-\gamma_p^2}\vartheta\left(\frac{1}{|\zeta|}\right), \tag{20}$$

so that series (18) will tend, to the first order in $1/|\zeta|$, towards a finite linear combination Σu_n of eigenvectors u_n.

It results from Eq. (18) that this linear combination Σu_n, which is itself an eigenvector associated with the same eigenvalue $-\gamma_n^2$, also verifies, to the first order in $1/|\zeta|$:

$$(k_n^2-\gamma_n^2)\int_V w_n\overline{\Sigma u_n}\,\mathrm{d}v+\mathrm{i}k\int_S\frac{w_n\overline{\Sigma u_n}}{\zeta}\,\mathrm{dS}=0, \tag{21}$$

allowing us to estimate the imaginary part of $-k_n^2$:

$$k_n^2 - \gamma_n^2 = -\mathrm{i}k \frac{\int_{S\cup F_1\cup F_2} (|\Sigma u_n|^2/\zeta)\,\mathrm{d}\gamma}{\int_V |\Sigma u_n|^2\,\mathrm{d}x} = -\frac{\mathrm{i}k}{\zeta_n}, \tag{22}$$

where ζ_n may be defined as the normalized impedance of the nth acoustic mode.

Therefore, resonance of system (9) occurs each time $k_n^2 = \gamma_n^2$. The smaller $R_e(1/\zeta)$ is, the more intense the resonance, and the narrower its pass band.

A simple application of the Green formula shows that every mode w_n of Eq. (15) verifies:

$$w_n(x) = -\int_{S\cup F_1\cup F_2} \left(\frac{\partial}{\partial n_y} - \frac{\mathrm{i}k}{\zeta}\right)\left(\frac{\mathrm{e}^{\mathrm{i}k_n|x-y|}}{4\pi|x-y|}\right) w_n(y)\,\mathrm{d}S(y). \tag{23}$$

The solution of Eq. (1) can thus be written as

$$\begin{aligned} p^i(x,k,\zeta,\varepsilon) &= \sum_{n=-\infty}^{n=+\infty} \alpha_n(k,\zeta,\varepsilon) w_n(x) \\ &= -\sum_{n=-\infty}^{n=+\infty} \alpha_n(k,\zeta,\varepsilon) \left(\frac{\partial}{\partial n_y} - \frac{\mathrm{i}k}{\zeta}\right)\left(\frac{\mathrm{e}^{\mathrm{i}k_n|x-y|}}{4\pi|x-y|}\right) w_n(y)\,\mathrm{d}S(y). \end{aligned} \tag{24}$$

But, always with a simple application of the Green formula to Eq. (9) and the Green kernel of an unlimited domain $\left(\mathrm{e}^{\mathrm{i}k|x-y|}/4\pi|x-y|\right)$:

$$\begin{aligned} p^i(x,k,\zeta,\varepsilon) = &-\int_{S\cup F_1\cup F_2} \left(\frac{\partial}{\partial n_y} - \frac{\mathrm{i}k}{\zeta}\right)\left(\frac{\mathrm{e}^{\mathrm{i}k|x-y|}}{4\pi|x-y|}\right) p^i(y,k,\zeta,\varepsilon)\,\mathrm{dS}(y) \\ &+ \int_S \frac{\mathrm{e}^{\mathrm{i}k|x-y|}}{4\pi|x-y|} \rho\omega^2(u(y,k,\varepsilon),n_y)\,\mathrm{dS}(y). \end{aligned} \tag{25}$$

It results directly from Eqs. (24) and (25) that

$$\begin{aligned} &\sum_{n=-\infty}^{n=+\infty} \alpha_n(k,\zeta,\varepsilon) \int_{S\cup F_1\cup F_2} \left(\left(\frac{\partial}{\partial n_y} - \frac{\mathrm{i}k}{\zeta}\right)\left(\frac{\mathrm{e}^{\mathrm{i}k|x-y|} - \mathrm{e}^{\mathrm{i}k_n|x-y|}}{4\pi|x-y|}\right)\right) w_n(y)\,\mathrm{dS}(y) \\ &\quad = \int_S \frac{\mathrm{e}^{\mathrm{i}k|x-y|}}{4\pi|x-y|} \rho\omega^2(u(y,k,\varepsilon),n_y)\,\mathrm{dS}(y). \end{aligned} \tag{26}$$

To compare

$$\sum_{n=-\infty}^{n=+\infty} \alpha_n(k,\zeta,\varepsilon) \int_{S\cup F_1\cup F_2} \left(\frac{\partial}{\partial n_y} - \frac{\mathrm{i}k}{\zeta}\right)\left(\frac{\mathrm{e}^{\mathrm{i}k_n|x-y|}}{4\pi|x-y|}\right) w_n(y)\,\mathrm{dS}(y) \tag{27}$$

with

$$\sum_{n=-\infty}^{n=+\infty} \alpha_n(k,\zeta,\varepsilon) \int_{S\cup F_1\cup F_2} \left(\frac{\partial}{\partial n_y} - \frac{\mathrm{i}k}{\zeta}\right)\left(\frac{\mathrm{e}^{\mathrm{i}k|x-y|}}{4\pi|x-y|}\right) w_n(y)\,\mathrm{dS}(y)$$
$$= \sum_{n=-\infty}^{n=+\infty} \alpha_n(k,\zeta,\varepsilon) \int_{S\cup F_1\cup F_2} \left(\frac{\partial}{\partial n_y} - \frac{\mathrm{i}k}{\zeta}\right)\left(\mathrm{e}^{\mathrm{i}(k-k_n)|x-y|}\frac{\mathrm{e}^{\mathrm{i}k_n|x-y|}}{4\pi|x-y|}\right) w_n(y)\,\mathrm{dS}(y)$$
$$= \sum_{n=-\infty}^{n=+\infty} \alpha_n(k,\zeta,\varepsilon) \int_{S\cup F_1\cup F_2} \left(\left(\mathrm{i}(k-k_n)\frac{\partial}{\partial n_y}|x-y|\right)\frac{\mathrm{e}^{\mathrm{i}k|x-y|}}{4\pi|x-y|}\right.$$
$$\left. + \left(\mathrm{e}^{\mathrm{i}(k-k_n)|x-y|}\right)\left(\frac{\partial}{\partial n_y} - \frac{\mathrm{i}k}{\zeta}\right)\left(\frac{\mathrm{e}^{\mathrm{i}k_n|x-y|}}{4\pi|x-y|}\right)\right) w_n(y)\,\mathrm{dS}(y), \tag{28}$$

let us note that the form of $\alpha_n(k,\zeta,\varepsilon)$ is

$$\alpha_n(k,\zeta,\varepsilon) = \sum_{m=-\infty}^{m=+\infty} \frac{k^2 \int_s \rho c^2 (e_m(y,k)\cdot n_y) w_n(y)\,\mathrm{dS}(y)}{(k_n+k)(k+\overline{k_m})} \frac{1}{(k_n-k)(k-k_m)}, \tag{29}$$

since $u(y,k,\varepsilon)$ represents the wall acceleration of an elastic shell. The coupling term of the mth structural mode with the acoustic fluid is included in $k_m = K_m - \mathrm{i}k\varepsilon_m$, where K_m is real.

Therefore, expressions (27) and (28) involve a double summation over the m and n indices.

Let $\Phi(k)$ be a smooth function. Let us compare the convolution by $\Phi(k)$ of the double summation terms in expression (27):

$$\{\Phi(k)\} \underset{k}{*} \left\{\alpha_{n,m}(k,\zeta,\varepsilon) \int_{S\cup F_1\cup F_2} \left(\frac{\partial}{\partial n_y} - \frac{\mathrm{i}k}{\zeta}\right)\left(\frac{\mathrm{e}^{\mathrm{i}k_n|x-y|}}{4\pi|x-y|}\right) w_n(y)\,\mathrm{dS}(y)\right\}$$
$$= \int_{k'=-\infty}^{k'=+\infty} \left\{\Phi(k-k')\alpha_{n,m}(k',\zeta,\varepsilon) \int_{S\cup F_1\cup F_2} \left(\frac{\partial}{\partial n_y} - \frac{\mathrm{i}k'}{\zeta}\right)\left(\frac{\mathrm{e}^{\mathrm{i}k_n|x-y|}}{4\pi|x-y|}\right) w_n(y)\,\mathrm{dS}(y)\right\} \mathrm{d}k'$$
$$= \oint \left\{\Phi(k-z)\alpha_{n,m}(z,\zeta,\varepsilon) \int_{S\cup F_1\cup F_2} \left(\frac{\partial}{\partial n_y} - \frac{\mathrm{i}z}{\zeta}\right)\left(\frac{\mathrm{e}^{\mathrm{i}k_n|x-y|}}{4\pi|x-y|}\right) w_n(y)\,\mathrm{dS}(y)\right\} \mathrm{d}z \tag{30}$$

with the convolution by $\Phi(k)$ of the double summation terms in expression (28), which can be written in an analogous way:

$$\oint \Phi(k-z)\alpha_{n,m}(z,\zeta,\varepsilon)$$
$$\times \int_{S\cup F_1\cup F_2} \left(\left(\mathrm{i}(z-k_n)\frac{\partial}{\partial n_y}|x-y|\right)\frac{\mathrm{e}^{\mathrm{i}\bar{z}|x-y|}}{4\pi|x-y|} + \left(\mathrm{e}^{\mathrm{i}(\bar{z}-k_n)|x-y|}\right)\left(\frac{\partial}{\partial n_y} - \frac{\mathrm{i}z}{\zeta}\right)\left(\frac{\mathrm{e}^{\mathrm{i}k_n|x-y|}}{4\pi|x-y|}\right)\right)$$
$$w_n(y)\,\mathrm{d}S(y)\Big\}\mathrm{d}z. \tag{31}$$

These convolutions are to be interpreted as mean values over a short frequency band.

The analytic functions under the integral signs are holomorphic out of the poles. The integration contour is a half-circle in the inferior half-plane completed with one diameter, sufficiently large so that the contribution of the circular sector can be neglected. It includes the poles $z = k_n$ with a negative imaginary part.

Let us use the residues theorem to perform the above comparison. The poles $z = k_n$ clearly appear in Eq. (17) and in the expression of $\alpha_n(k, \zeta, \varepsilon)$ given by Eq. (29). The poles $z = k_m$, due to $u(y, k, \varepsilon)$, also appear in Eq. (29) and represent a resonance of the structure coupled with the fluid.

For a given wavenumber k, the terms in the double summations which will contribute in a non-negligible way to the results are those for which:

$$\begin{aligned} k - k_n &= \vartheta\left(\frac{1}{\zeta_n}\right), \\ k - k_m &= \vartheta(\varepsilon_m), \\ k_n - k_m &= \vartheta\left(\frac{1}{\zeta_n}, \varepsilon_m\right). \end{aligned} \tag{32}$$

We thus obtain, for Eqs. (30) and (31), respectively:

$$\begin{aligned} &\vartheta\left(\frac{1}{\zeta}, \varepsilon\right) + \rho c^2 \int_{S\cup F_1\cup F_2} \left(\frac{\partial}{\partial n_y} - \frac{\mathrm{i}k}{\zeta}\right)\left(\frac{\mathrm{e}^{\mathrm{i}k_n|x-y|}}{4\pi|x-y|}\right)\frac{w_n(y)}{(k_n - k_m)}\,\mathrm{d}S(y) \\ &\quad\times\left(\frac{k_n^2\Phi(k-k_n)\int_S(e_m(y,k_n),n_y)w_n(y)\,\mathrm{d}S(y)}{(k_n+k_n)(k_n+\overline{k_m})} + \frac{k_m^2\Phi(k-k_m)\int_S(e_m(y,k_m),n_y)w_n(y)\,\mathrm{d}S(y)}{(k_n+k_m)(k_m+\overline{k_m})}\right) \end{aligned} \tag{33}$$

and

$$\begin{aligned} &\vartheta\left(\frac{1}{\zeta}, \varepsilon\right) + \rho c^2 \int_{S\cup F_1\cup F_2} \left(\frac{\partial}{\partial n_y} - \frac{\mathrm{i}k}{\zeta}\right)\left(\frac{\mathrm{e}^{\mathrm{i}k_n|x-y|}}{4\pi|x-y|}\right)\frac{w_n(y)}{(k_n - k_m)}\,\mathrm{d}S(y) \\ &\quad\times\left(\frac{k_n^2\Phi(k-k_n)\mathrm{e}^{\mathrm{i}(\overline{k_n}-k_n)|x-y|}\int_S(e_m(y,k_n),n_y)w_n(y)\,\mathrm{d}S(y)}{(k_n+k_n)(k_n+\overline{k_m})}\right. \\ &\quad\left.+\frac{k_m^2\Phi(k-k_m)\mathrm{e}^{\mathrm{i}(\overline{k_m}-k_n)|x-y|}\int_S(e_m(y,k_m),n_y)w_n(y)\,\mathrm{d}S(y)}{(k_n+k_m)(k_m+\overline{k_m})}\right) \\ &\quad-\rho c^2\int_{S\cup F_1\cup F_2}\frac{\mathrm{i}\partial(|x-y|)}{\partial n_y}\frac{\mathrm{e}^{\mathrm{i}\overline{k_m}|x-y|}}{4\pi|x-y|}w_n(y)\,\mathrm{d}S(y)\left(\frac{k_m^2\Phi(k-k_m)\int_S(e_m(y,k_m),n_y)w_n(y)\,\mathrm{d}S(y)}{(k_n+k_m)(k_m+\overline{k_m})}\right). \end{aligned} \tag{34}$$

We are only interested in resonance peaks and sufficiently high wavenumbers. Under these conditions, the term in the third line of Eq. (34) becomes doubly negligible, on the one hand, because it is not affected by a resonance (sharper when ε and$1/\zeta$ tend to 0), and on the other hand, because its order in k, k_n, k_m is 0.

Therefore, we may consider that the term under the integration sign of Eq. (34) is simply related to that of Eq. (33) by a multiplicative term:

$$\left(\frac{k_n^2\Phi(k-k_n)\mathrm{e}^{\mathrm{i}(\overline{k_n}-k_n)|x-y|}\int_\Gamma e_m(y,k_n)w_n(y)\,\mathrm{d}\gamma(y)}{(k_n+k_n)(k_n+\overline{k_m})}\right.$$
$$\left.+\frac{k_m^2\Phi(k-k_m)\mathrm{e}^{\mathrm{i}(\overline{k_m}-k_n)|x-y|}\int_\Gamma e_m(y,k_n)w_n(y)\,\mathrm{d}\gamma(y)}{(k_n+k_m)(k_m+\overline{k_m})}\right)^{-1}$$
$$\times\left(\frac{k_n^2\Phi(k-k_n)\int_\Gamma e_m(y,k_n)w_n(y)\,\mathrm{d}\gamma(y)}{(k_n+k_n)(k_n+\overline{k_m})}+\frac{k_m^2\Phi(k-k_m)\int_\Gamma e_m(y,k_n)w_n(y)\,\mathrm{d}\gamma(y)}{(k_n+k_m)(k_m+\overline{k_m})}\right). \tag{35}$$

It is always possible to choose the function $\Phi(k)$ as a window constant over a sufficiently narrow band in order to consider that $e_m(y,k)$ does not evolve inside it. In this narrow band, the imaginary and real parts of $k, k_n, \overline{k_n}, k_m, \overline{k_m}, \gamma_n$ for the terms which contribute in a non-negligible way to the results become very close when $\zeta_n \to \infty, \varepsilon_m \to 0$. We can thus write

$$\frac{k_n^2}{(k_n+k_n)(k_n+\overline{k_m})} \cong \frac{k_m^2}{(k_n+k_m)(k_n+\overline{k_m})} \cong \frac{1}{4},$$
$$\overline{k_m}-k_n = K_m-\gamma_n+\mathrm{i}\left(k\varepsilon_m+\frac{k}{k_n+\gamma_n}\frac{1}{\zeta_n}\right) \cong \mathrm{i}\left(k\varepsilon_m+\frac{1}{2\zeta_n}\right),$$
$$\overline{k_n}-k_n = \frac{\mathrm{i}k}{k_n+\overline{k_n}}\left(\frac{1}{\zeta_n}+\frac{1}{\overline{\zeta_n}}\right) \cong \mathrm{i}R_e\left(\frac{1}{\zeta_n}\right),$$
$$\mathrm{e}^{\mathrm{i}(\overline{k_m}-k_n)|x-y|} \cong \mathrm{e}^{-\left(k\varepsilon_m+\frac{1}{2\zeta_n}\right)|x-y|}. \tag{36}$$

A simplifying hypothesis consists in considering that the above multiplicative factor does not depend upon m and n indices and is

$$\left(\mathrm{e}^{-R_e(1/\zeta)|x-y|}+\mathrm{e}^{-(k\varepsilon+(1/2\zeta))|x-y|}\right)^{-1}. \tag{37}$$

This relevant hypothesis for defining a worthwhile dissipation model allows us to recombine all the modes in the equation obtained after a convolution by $\Phi(k)$ of both sides of Eq. (26), which yields the following:

First intermediary result—Integral relation between wall pressure and acceleration

$$\int_{S\cup F_1\cup F_2}\left(1-\left(\mathrm{e}^{-R_e(1/\zeta)|x-y|}+\mathrm{e}^{-(k\varepsilon+(1/2\zeta))|x-y|}\right)^{-1}\right)\left(\frac{\partial}{\partial n_y}-\frac{\mathrm{i}k}{\zeta}\right)\left(\frac{\mathrm{e}^{\mathrm{i}k|x-y|}}{4\pi|x-y|}\right)p^i(y,k)\,\mathrm{d}S(y)$$
$$\underset{k}{=}\int_S\frac{\mathrm{e}^{\mathrm{i}k|x-y|}}{4\pi|x-y|}\rho\omega^2(u(y,k),n_y)\,\mathrm{d}S(y)+\vartheta\left(\frac{1}{\zeta},\varepsilon\right). \tag{38}$$

Hereafter, for the sake of simplicity, we will omit the $\vartheta\left(\frac{1}{\zeta},\varepsilon\right)$ term and the convolution over k, which will be implicit in all the equations written below, and we will assume that ζ is strictly real.

4.1.1. Physical interpretation of result (38)

When $1/\zeta$ is small enough, everything occurs inside the cavity as if the wall were quite rigid as regards reflection of the waves. The energy introduced by the motion of the wall is dissipated both acoustically at the wall and in the structure. The integral relation (38) sums up this behaviour in mean value.

4.1.2. Remarks on modal expansion inside the cavity

It may seem irrelevant that the pressure inside the cavity, even to the first order in $1/\zeta$, is a sum of modes w_n, since each one verifies a homogeneous boundary condition:

$$\left(\frac{\partial w_n}{\partial n} - \frac{\mathrm{i}k}{\zeta} w_n\right)\bigg|_{S\cup F_1\cup F_2} = 0, \tag{39}$$

so that the sum verifies such a homogeneous condition instead of

$$\left(\frac{\partial p^i}{\partial n} - \frac{\mathrm{i}k}{\zeta} p^i\right)\bigg|_S = \rho\omega^2(u(y,k,\varepsilon)n_y). \tag{40}$$

In fact, Eq. (17) results from the convolution of a Green function with a wall source term. This Green function has a singularity at the location of the Dirac distribution. Its modal expansion cannot converge at that location, even if the result of the convolution strongly converges.

Thus, the derivation of the resulting expression cannot be made by a simple derivation of the Green function under the integral sign, which would correspond to the derivation of the series term by term.

Indeed,

$$\left(\frac{\partial p^i}{\partial n} - \frac{\mathrm{i}k}{\zeta} p^i\right)\bigg|_S \neq \int_S \left(\frac{\partial G^\zeta}{\partial n} - \frac{\mathrm{i}k}{\zeta} G^\zeta\right)\rho\omega^2(u(y,k),n_y)\,\mathrm{d}S = 0, \tag{41}$$

because of the boundary condition verified by the Green function. Actually, the derivation must be achieved in a distribution sense and concretely obtained by excluding a disk centred at the location of the Dirac distribution [30b].

Nevertheless, since the resulting expressions strongly converge even at the wall, the modal expansion is suitable, provided its normal derivative is avoided.

A formulation with Dirichlet modes (the Green function null on the wall) could have been studied, but would have certainly been less tractable because of the derivation to be performed.

4.2. The stationary phase method for localizing noise provenance (second argument)

In all the above expressions, the normal derivative of the Green kernel of an unlimited domain ($\mathrm{e}^{\mathrm{i}k|x-y|}/4\pi|x-y|$) is

$$\frac{\partial}{\partial n_y}\left(\frac{\mathrm{e}^{\mathrm{i}k|x-y|}}{4\pi|x-y|}\right) = \frac{\mathrm{e}^{\mathrm{i}k|x-y|}}{4\pi|x-y|}\left[\left(\mathrm{i}k - \frac{1}{|x-y|}\right)\frac{(y-x,n_y)}{|x-y|}\right]. \tag{42}$$

When x is a point of the axis inside an axisymmetric enclosure, $|x-y|$ retains the same value when y runs on a same parallel of latitude. So does $(y-x,n_y)$. Thus, $(e^{ik|x-y|}/4\pi|x-y|)$ and $(\partial/\partial n_y)(e^{ik|x-y|}/4\pi|x-y|)$ remain constant on a parallel of latitude.

In consequence, the integrations in Eq. (25) can be transformed into integrations on the meridian line.

Calling M a meridian line, $d\mu(y)$ its infinitesimal length, y the running abscissa on this line, θ the azimuth and $f(y,\theta)$ any integrand:

$$\int_S f(y,\theta)\,dS(y,\theta)=\int_M\left(\int_{\theta=0}^{2\pi} f(y,\theta)\,d\theta\right)d\mu(y)=\int_M F(y)\,d\mu(y). \tag{43}$$

$F(y)$ is the zero-order azimuthal component of the function $f(y,\theta)$, which, as a 2π periodic function of θ, can be expanded in an azimuthal series:

$$2\pi f(y,\theta)=F(y)+\sum_{l\neq 0} f_l(y)e^{il\theta}. \tag{44}$$

Let us retain the same notation for the surface and the meridian line and use a capital letter for the zero-order azimuthal component. When x is an axis point, instead of Eqs. (38) and (37), we can write, respectively:

$$\begin{aligned} p^i(x,k,\zeta,\varepsilon)=&-\int_{S\cup F_1\cup F_2}\left(\frac{\partial}{\partial n_y}-\frac{ik}{\zeta}\right)\left(\frac{e^{ik|x-y|}}{4\pi|x-y|}\right)P^i(y,k,\zeta,\varepsilon)\,dS(y)\\ &+\int_S\frac{e^{ik|x-y|}}{4\pi|x-y|}\rho\omega^2(U(y,k,\varepsilon),n_y)\,dS(y), \end{aligned} \tag{45}$$

$$\begin{aligned} &\int_{S\cup F_1\cup F_2}\left(1-\left(e^{-|x-y|/\zeta}+e^{-(k\varepsilon+1/2\zeta)|x-y|}\right)^{-1}\right)\left(\frac{\partial}{\partial n_y}-\frac{ik}{\zeta}\right)\left(\frac{e^{ik|x-y|}}{4\pi|x-y|}\right)P^i(y,k,\zeta,\varepsilon)\,d\mu(y)\\ &\quad=\int_S\frac{e^{ik|x-y|}}{4\pi|x-y|}\rho\omega^2(U(y,k,\varepsilon),n_y)\,d\mu(y). \end{aligned} \tag{46}$$

The combination of Eqs. (45) and (46) gives:

$$\begin{aligned} p^i(x,k,\zeta,\varepsilon)=&-\int_{S\cup F_1\cup F_2}(e^{-|x-y/\zeta}+e^{-(k\varepsilon+1/2\zeta)|x-y|})^{-1}\left(\frac{\partial}{\partial n_y}-\frac{ik}{\zeta}\right)\left(\frac{e^{ik|x-y|}}{4\pi|x-y|}\right)\\ &\times P^i(y,k,\zeta,\varepsilon)\,dS(y). \end{aligned} \tag{47}$$

Let α be a running parameter for the points $y(\alpha)$ of the meridian line.

Define φ and d functions:

$$|x-y(\alpha)|=d(\alpha), \tag{48}$$

$$d\mu(y(\alpha))=\mu(\alpha)\,d(\alpha), \tag{49}$$

where x is the axis point on which the pressure is to be computed.

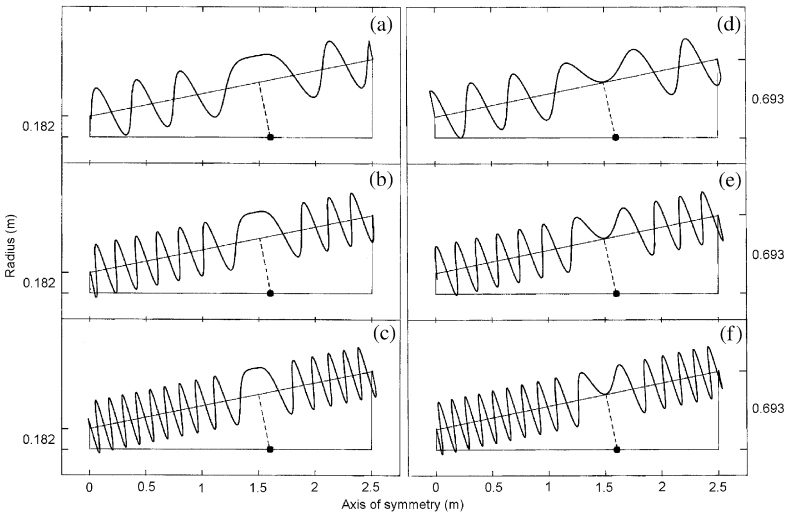

Fig. 2. Plot of $e^{-ikd(\alpha_0)}e^{ikd(\alpha)}$ on a truncated cone meridian for three frequencies. (a)–(c) real part; (d)–(f) imaginary part. Frequencies: (a), (d), 500 Hz; (b), (e), 1000 Hz; (c), (f) 3000 Hz.

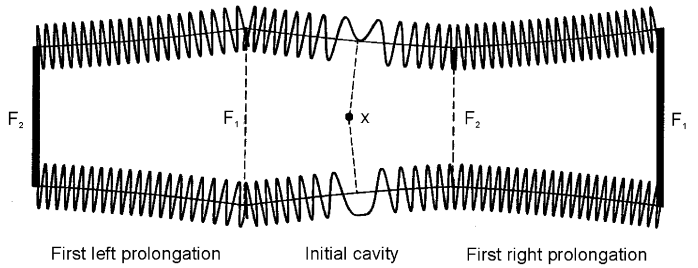

Fig. 3. Extension of problem (9) with respect to the rigid ends F_1 and F_2. Top: plot of $\sin(k(d(\alpha)-d(\alpha_0)))$. Bottom: plot of $\cos(k(d(\alpha)-d(\alpha_0)))$.

The integrals in expressions (45), (46) and (47) have the form:

$$\int_M e^{ikd(\alpha)}\psi(\alpha)\,d\alpha. \tag{50}$$

When k tends to infinity, $e^{ikd(\alpha)}$ becomes highly oscillating outside the zones in which $d(\alpha)$ is stationary, that is to say:

$$\frac{\partial d(\alpha)}{\partial \alpha} = 0. \tag{51}$$

Fig. 2 shows this better than mathematical arguments. The represented structure is a truncated cone closed by two rigid ends. Its dimensions are indicated in meters. It has been used in a

reverberant room for an experiment, which will be discussed below to compare a theoretical calculation with the experimental results. In this particular case, for each axis point, there is only one point $y(\alpha_0)$ where the distance $d(\alpha) = |x - y(\alpha)|$ is stationary (minimal).

The real and imaginary parts of $e^{-ikd(\alpha_0)}e^{ikd(\alpha)}$ were plotted on the meridian curve for three frequencies (500, 1000, 3000 Hz).

Stationary lobes clearly appear.

It will be assumed that there is always a finite number of such stationary points α_j, thus defining J contributing zones μ_j. This excludes the case of a sphere where there are only stationary distance points when x is the centre of the sphere, a case in which all the derivatives verify: $(\partial^m d/\partial\alpha^m)(\alpha) = 0$, whatever the values of α and m.

Another point to be noted is that, in expressions (45)–(47), some integrations are performed on $S \cup F_1 \cup F_2$, and others on S only. In fact the integration over $S \cup F_1 \cup F_2$ is not necessary, since Eq. (9) can easily be extended by symmetry.

For instance, let us assume that the initial cavity has been extended with two similar cavities on which the motions of the flexible portions are exactly the same, but symmetrical with respect to the ends F_1 and F_2, as shown in Fig. 3.

The pressure inside the initial cavity will not be modified if the intermediary ends F_1 and F_2 are suppressed. Actually, all the internal points x of the initial cavity are outside the appended cavities. The Green relation thus gives 0 at x for an added cavity:

$$0 = -\int_{S_a^f}\left(\frac{\partial}{\partial n_y} - \frac{ik}{\zeta}\right)\left(\frac{e^{ik|x-y|}}{4\pi|x-y|}\right)p^i(y,k,\varsigma,\varepsilon)\,dS(y) + \int_{S_a}\frac{e^{ik|x-y|}}{4\pi|x-y|}\rho\omega^2(u(y,k,\varepsilon),n_y)\,dS(y), \tag{52}$$

where S_a^f is the edge of an appended cavity constituted of a surface S_a (identical to S) closed by two rigid ends (identical to F_1 and F_2).

Calling $\cup$ the reunion of initial and added surfaces and recalling that ζ is infinite valued on $F_1 \cup F_2$, we can write:

$$p^i(x,k,\varsigma,\varepsilon) = -\int_{\cup_a S_a^f}\left(\frac{\partial}{\partial n_y} - \frac{ik}{\zeta}\right)\left(\frac{e^{ik|x-y|}}{4\pi|x-y|}\right)p^i(y,k,\varsigma,\varepsilon)\,dS(y) + \int_{\cup_a S_a}\frac{e^{ik|x-y|}}{4\pi|x-y|}\left(\rho\omega^2(u(y,k,\varepsilon),n_y)\right)dS(y). \tag{53}$$

Since the sums over two adjacent ends cancel each other out because the normal vectors have opposite signs, we can write

$$p^i(x,k,\zeta,\varepsilon) = -\int_{F_1\cup(\cup_a S_a)\cup F_2}\left(\frac{\partial}{\partial n_y} - \frac{ik}{\zeta}\right)\left(\frac{e^{ik|x-y|}}{4\pi|x-y|}\right)p^i(y,k,\zeta,\varepsilon)\,dS(y) + \int_{\cup_a S_a}\frac{e^{ik|x-y|}}{4\pi|x-y|}\rho\omega^2(u(y,k,\varepsilon),n_y)\,dS(y). \tag{54}$$

The process can be reiterated as many times as needed, which comes to pushing back the ends as far as wanted [30c].

Obviously, the integration has to be performed not only on the initial surface but also over all S_a surfaces.

However, the stationary phase zones will stay at the same place on the edge of the new cavity, as shown by the plot of $e^{-ikd(\alpha_0)}e^{ikd(\alpha)}$ in Fig. 3.

Hence, we can legitimately neglect the effects of the ends F_1 and F_2, most likely of the second order, which probably compensate for the contribution of the edges of the definition domain of parameter α, neglected up till now.

Let us therefore assume that the stationary phase method can be applied.

One could use the formulae derived from this method, but it is not actually necessary. It is sufficient to recall that $|x-y(\alpha)| = d(\alpha)$ does not evolve inside each of the J stationary lobes, so that Eqs. (46) and (47) can be written, respectively, as

$$\sum_j \left(1 - \left(e^{-d(\alpha_j)/\zeta} + e^{-(k\varepsilon+(1/2\zeta))d(\alpha_j)}\right)^{-1}\right)\left(ik - \frac{1}{d(\alpha_j)} - \frac{ik}{\zeta}\right)\int_{\mu_j} \frac{e^{ik|x-y|}}{4\pi|x-y|} P^i(y,k,\zeta,\varepsilon)\,d\mu(y)$$
$$= \sum_j \int_{\mu_j} \frac{e^{ik|x-y|}}{4\pi|x-y|}\rho\omega^2(U(y,k,\varepsilon),n_y)\,d\mu(y), \tag{55}$$

$$p^i(x,k,\zeta,\varepsilon) = -\sum_j \left(e^{-d(\alpha_j)/\zeta} + e^{-(k\varepsilon+(1/2\zeta))d(\alpha_j)}\right)^{-1} \times \left(ik - \frac{1}{d(\alpha_j)} - \frac{ik}{\zeta}\right)\int_{\mu_j} \frac{e^{ik|x-y|}}{4\pi|x-y|} P^i(y,k,\zeta,\varepsilon)\,d\mu(y). \tag{56}$$

In these two equations, we have used the relation:

$$\left(y(\alpha_j) - x, n_{y(\alpha_j)}\right) = \left|x - y(\alpha_j)\right| = d(\alpha_j), \tag{57}$$

valid for a stationary point $y(\alpha)$ [30d].

There are two axis stationary phase points for the integration over $P^i(y,k,\zeta,\varepsilon)$. Nevertheless, as ζ is infinite valued on $F_1 \cup F_2$, their contributions in expression (55) tend towards zero by pushing back F_1 and F_2 to infinity as mentioned above.

When, for an axis point x, there is only one stationary phase point ($\alpha = \alpha_0$)—which is generally the case—the final expression is particularly simple because the contribution of wall acceleration only comes from one parallel of latitude, using after [32]:

$$\lim_{k\to\infty} \int_{-\infty}^{+\infty} e^{ikd(\alpha)}\psi(\alpha)\,d\alpha = \frac{(2\pi)^{\frac{1}{2}}e^{i\pi/4}}{\left[k\frac{\partial^2 d}{\partial^2\alpha}\Big|_{\alpha_0}\right]^{\frac{1}{2}}}\psi(\alpha_0)e^{ikd(\alpha_0)}. \tag{58}$$

Thanks to Eq. (58), the integral expressions in Eq. (55) become a simple equality at the stationary point specified by α_0, which can be introduced into Eq. (56) to give:

$$p^i(x,k,\zeta,\varepsilon) = \left(1 - \left(\mathrm{e}^{-d(\alpha_0)/\zeta} + \mathrm{e}^{-\left(k\varepsilon+(1/2\zeta)\right)d(\alpha_0)}\right)\right)^{-1} \int_{\mu_0} \frac{\mathrm{e}^{\mathrm{i}k|x-y|}}{4\pi|x-y|}\rho\omega^2(U(y,k,\varepsilon),n_y)\,\mathrm{d}\mu(y)$$
$$= \int_S \left(1 - \left(\mathrm{e}^{-|x-y|/\zeta} + \mathrm{e}^{-\left(k\varepsilon+(1/2\zeta)\right)|x-y|}\right)\right)^{-1} \frac{\mathrm{e}^{\mathrm{i}k|x-y|}}{4\pi|x-y|}\rho\omega^2(U(y,k,\varepsilon),n_y)\,\mathrm{d}\mu(y), \quad (59)$$

when $\left.\frac{\partial^2 d}{\partial^2\alpha}\right|_{\alpha_0} \neq 0$.

However, Eq. (59) remains true when, for J distinct points $x^{j'}$ at least, the main contributions in each of the J corresponding Eq. (55) come from J parallels of latitude $\mu_j^{j'}$ of the surface S where the distance $|x^{j'} - y(\alpha_j^j)| = d(\alpha_j^{j'})$ is stationary.

Indeed, using Eq. (58) for each zone $\mu_j^{j'}$, Eq. (55) can be transformed into

$$0 = \left(\frac{2\pi}{k}\right)^{\frac{1}{2}} \mathrm{e}^{\frac{\mathrm{i}\pi}{4}} \sum_j \frac{\mathrm{e}^{\mathrm{i}kd(\alpha_j^{j'})}\mu(\alpha_j^{j'})}{d(\alpha_j^{j'})\left[\left.\frac{\partial^2 d}{\partial\alpha^2}\right|_{\alpha_j^{j'}}\right]^{\frac{1}{2}}} \times \left(\left(1 - \left(\mathrm{e}^{-d(\alpha_j^{j'})/\zeta} + \mathrm{e}^{-\left(k\varepsilon+(1/2\zeta)\right)d(\alpha_j^{j'})}\right)^{-1}\right)\right.$$
$$\left. \times \left(\mathrm{i}k - \frac{1}{d(\alpha_j^{j'})} - \frac{\mathrm{i}k}{\zeta}\right) P^i(y(\alpha_j^{j'}),k,\zeta,\varepsilon) - \rho\omega^2\left(U(y(\alpha_j^{j'}),k,\varepsilon),n_{y\left(\alpha_j^{j'}\right)}\right)\right). \quad (60)$$

If the determinant in $\alpha_j^{j'}$ below is different from 0:

$$\left|\frac{\mathrm{e}^{\mathrm{i}kd(\alpha_j^{j'})}\mu(\alpha_j^{j'})}{d(\alpha_j^{j'})\left[\left.\frac{\partial^2 d}{\partial\alpha^2}\right|_{\alpha_j^{j'}}\right]}\right| \neq 0, \quad (61)$$

the equality between pressure and wall acceleration can still be written locally as

$$\left(1 - \left(\mathrm{e}^{-d(\alpha_j^{j'})/\zeta} + \mathrm{e}^{-\left(k\varepsilon+(1/2\zeta)\right)d(\alpha_j^{j'})}\right)^{-1}\right)\left(\mathrm{i}k - \frac{1}{d(\alpha_j^{j'})} - \frac{\mathrm{i}k}{\zeta}\right) P^i(y(\alpha_j^{j'}),k,\zeta,\varepsilon)$$
$$= \rho\omega^2\left(U(y(\alpha_j^{j'}),k,\varepsilon),n_{y\left(\alpha_j^{j'}\right)}\right), \quad (62)$$

and introduced in Eq. (56) to give again Eq. (59):

$$p^i(x,k,\zeta,\varepsilon) = \sum_j \left(1 - \left(\mathrm{e}^{-d(\alpha_j)/\zeta} + \mathrm{e}^{-\left(k\varepsilon+(1/2\zeta)\right)d(\alpha_j)}\right)\right)^{-1} \int_{\mu_j} \frac{\mathrm{e}^{\mathrm{i}k|x-y|}}{4\pi|x-y|}\rho\omega^2(U(y,k,\varepsilon),n_y)\,\mathrm{d}\mu(y)$$
$$= \int_S \left(1 - \left(\mathrm{e}^{-|x-y|/\zeta} + \mathrm{e}^{-\left(k\varepsilon+(1/2\zeta)\right)|x-y|}\right)\right)^{-1} \frac{\mathrm{e}^{\mathrm{i}k|x-y|}}{4\pi|x-y|}\rho\omega^2(U(y,k,\varepsilon),n_y)\,\mathrm{d}\mu(y). \quad (63)$$

It remains to be determined when the stationary phase method is applicable, i.e. which functions $\psi(\alpha)$ in expression (50) appear to be smooth in comparison with the highly oscillating behaviour of the complex exponential.

When the frequency tends to infinity, the structural wavelengths evolve, for axisymmetric modes, like the power $\frac{1}{2}$ of the acoustic wavenumber [30e], and they will appear to be infinitely greater than the acoustic wavelength associated with the oscillations of $e^{ikd(\alpha)}$: above the coincidence frequency, structural modes are acoustically fast and the stationary phase method will be suitable for the acceleration terms of Eqs. (45) and (46).

But this acceleration term $\rho\omega^2(U(y,k,\varepsilon),n_y)$ is also smoothly variable for most aeronautical airborne structures in comparison with $e^{ikd(\alpha)}$, as soon as the frequency is higher than the first axisymmetric mode frequency of the structure in vacuo.

Indeed, as already indicated, only axisymmetric structural modes contribute to the pressure on the axis. In addition, the curvature strongly increases the rigidity of most aeronautical airborne structures, as explained in Ref. [30f] with reference to Ref. [33].

Two consequences of this curvature effect on axisymmetric modes concur to make the stationary phase method suitable for developing the integral term containing the wall acceleration in Eqs. (45) and (46) for such structures:

- the first axisymmetric mode of the structure in vacuo is sufficiently high for the asymptotic expansion to be relevant;
- the wavelengths of all the structure axisymmetric modes are longer than the acoustic wavelength, even below the coincidence frequency (the axisymmetric modes of such structures are always acoustically fast).

Nevertheless, a graphic method is given in Ref. [30g] to verify the applicability of the stationary phase method when it has to be treated with caution.

As regards acoustics, structural axisymmetric modes only excite the acoustic axisymmetric modes when their trace on the wall matches the structural acceleration. The wavelengths of the wall pressure oscillations are as long as those of the structure vibrations.

This is not in contradiction with the fact that in a sphere, the diameter of which is an acoustic wavelength, there is necessarily at least one surface of nodes [30h]. This simply means that the nodes of the excited axisymmetric acoustic modes are more concentrated perpendicularly to the wall than tangentially.

Therefore, the integral expressions (45)–(47), containing both the pressure and wall acceleration terms, can all be developed through the stationary phase method to derive Eq. (63). This can be performed at any frequency for most aeronautical airborne structures, since the structure acts as a frequency filter, which practically eliminates any response below its lowest natural frequency.

Let us now recall the second intermediary result.

Second intermediary result—Expression of the cavity axis pressure

$$p^i(x,k,\zeta,\varepsilon)=\int_S\left(1-\left(e^{-|x-y|/\zeta}+e^{-\left(k\varepsilon+(1/2\zeta)\right)|x-y|}\right)\right)^{-1}\frac{e^{ik|x-y|}}{4\pi|x-y|}\rho\omega^2(U(y,k,\varepsilon),n_y)\,d\mu(y). \quad (64)$$

Noise on the axis generally comes from a particular parallel of latitude, the parallel constituted by the points nearest to this axis point.

4.2.1. Remark

The stationary phase lobe width is of the same order in k as the structure wavelength [30g]. This is not a problem since the significant point is that the contribution outside the lobes tends to zero when k tends to infinity. It is better to keep the integration on the whole lobes—or roughly on the whole surface S—instead of using a relation such as Eq. (58).

5. Fluid–structure coupling (third argument)

When x is an axis point inside the cavity, the integral relation:

$$0 = \int_{S\cup F_1\cup F_2} \frac{e^{ik|x-y|}}{4\pi|x-y|}\left(ik - \frac{1}{|x-y|}\right)\frac{(y-x,n_y)}{|x-y|}P^e(y,k)\,d\mu(y) - \int_S \frac{e^{ik|x-y|}}{4\pi|x-y|}\rho\omega^2(U(y,k,\varepsilon),n_y)\,d\mu(y) \tag{65}$$

can be obtained through the Green theorem applied to the external equation (11).

For the same reasons as in 4.2.:

- the stationary phase method is suitable for developing the integral expression (65);
- the extension of the problem by symmetry with respect to the rigid ends allows us to avoid integration over these ends.

Thus, the main contributions in expression (65) come from the same parallels of latitude μ_j of the surface S where the distance $|x-y(\alpha_j)| = d(\alpha_j)$ is stationary. If we add hypothesis (61), we obtain

$$0 = \sum_j\left(\left(ik - \frac{1}{d(\alpha_j)}\right) - i\frac{k}{\zeta}\right)\int_{\mu_j}\frac{e^{ik|x-y|}}{4\pi|x-y|}P^e(y,k)\,d\mu(y) - \sum_j\frac{\left(ik-\frac{1}{d(\alpha_j)}\right)-i\frac{k}{\zeta}}{\left(ik-\frac{1}{d(\alpha_j)}\right)}\int_{\mu_j}\frac{e^{ik|x-y|}}{4\pi|x-y|}\rho\omega^2(U(y,k,\varepsilon),n_y)\,d\mu(y), \tag{66}$$

which can also be written, again thanks to hypothesis (61), as

$$\int_{S\cup F_1\cup F_2}\left(\frac{\partial}{\partial n_y} - \frac{ik}{\zeta}\right)\left(\frac{e^{ik|x-y|}}{4\pi|x-y|}\right)P^e(y,k)d\mu(y) = \int_S\left(1 - \frac{\frac{ik}{\zeta}}{ik-\frac{1}{|x-y|}}\right)\frac{e^{ik|x-y|}}{4\pi|x-y|}\rho\omega^2(U(y,k,\varepsilon),n_y)\,d\mu(y). \tag{67}$$

With the same considerations as above, we can write Eq. (46) as

$$\int_{S\cup F_1\cup F_2}\left(\frac{\partial}{\partial n_y}-\frac{\mathrm{i}k}{\zeta}\right)\left(\frac{\mathrm{e}^{\mathrm{i}k|x-y|}}{4\pi|x-y|}\right)P^i(y,k,\zeta,\varepsilon)\,\mathrm{d}\mu(y)$$
$$=\int_S\left(1+\left(\mathrm{e}^{-|x-y|/\zeta}+\mathrm{e}^{-(k\varepsilon+(1/2\zeta))|x-y|}-1\right)^{-1}\right)\frac{\mathrm{e}^{\mathrm{i}k|x-y|}}{4\pi|x-y|}\rho\omega^2(U(y,k,\varepsilon),n_y)\,\mathrm{d}\mu(y). \quad (68)$$

The subtraction of Eq. (67) from Eq. (68) leads to another expression of the pressure inside the cavity:

$$\int_{S\cup F_1\cup F_2}\left(\frac{\partial}{\partial n_y}-\frac{\mathrm{i}k}{\zeta}\right)\left(\frac{\mathrm{e}^{\mathrm{i}k|x-y|}}{4\pi|x-y|}\right)[P(y,k,\zeta,\varepsilon)]\,\mathrm{d}\mu(y)$$
$$=\int_S\left(\frac{\frac{\mathrm{i}k}{\zeta}}{\mathrm{i}k-\frac{1}{|x-y|}}+\left(\mathrm{e}^{-|x-y|/\zeta}+\mathrm{e}^{-(k\varepsilon+(1/2\zeta))|x-y|}-1\right)^{-1}\right)\frac{\mathrm{e}^{\mathrm{i}k|x-y|}}{4\pi|x-y|}\rho\omega^2(U(y,k,\varepsilon),n_y)\,\mathrm{d}\mu(y), \quad (69)$$

where $[P(y,k,\zeta,\varepsilon)]=\left(P^i(y,k,\zeta,\varepsilon)-P^e(y,k)\right)\big|_{S\cup F_1\cup F_2}$ is the wall-pressure jump between interior and exterior cavity.

Let

$$\left(\left(\mathrm{i}k-\frac{1}{|x-y|}\right)\frac{(y-x,n_y)}{|x-y|}-\frac{\mathrm{i}k}{\zeta}\right)\mathrm{d}\mu(y)=\varphi_P(\alpha)\mu(\alpha)\,\mathrm{d}\alpha,$$
$$\left(\frac{\frac{\mathrm{i}k}{\zeta}}{\mathrm{i}k-\frac{1}{|x-y|}}+\left(e^{-|x-y|/\zeta}+e^{-(k\varepsilon+(1/2\zeta))|x-y|}-1\right)^{-1}\right)\rho\omega^2\,\mathrm{d}\mu(y)=\varphi_U(\alpha)\mu(\alpha)\,\mathrm{d}\alpha. \quad (70)$$

With the same considerations used for establishing Eq. (64) through the transformation of Eq. (55) into Eq. (60), instead of Eq. (69), we can write

$$\left(\frac{2\pi}{k}\right)^{\frac{1}{2}}\mathrm{e}^{\frac{\mathrm{i}\pi}{4}}\sum_j\frac{\mathrm{e}^{\mathrm{i}kd(\alpha_j^{j'})}\mu(\alpha_j^{j'})}{d(\alpha_j^{j'})\left[\frac{\partial^2 d}{\partial\alpha^2}\Big|_{\alpha_j^{j'}}\right]^{\frac{1}{2}}}\left(\varphi_P(\alpha_j^{j'})\left[P(y(\alpha_j^{j'}),k,\zeta,\varepsilon)\right]-\varphi_U(\alpha_j^{j'})\left(U(y(\alpha_j^{j'}),k,\varepsilon),n_{y\left(\alpha_j^{j'}\right)}\right)\right)=0. \quad (71)$$

Therefore, using the same hypothesis (61), the coupling is purely local:

$$\left[P(y(\alpha_j^{j'}),k,\zeta,\varepsilon)\right]=\frac{\varphi_U(\alpha_j^{j'})}{\varphi_P(\alpha_j^{j'})}\left(U(y(\alpha_j^{j'}),k,\varepsilon),n_{y\left(\alpha_j^{j'}\right)}\right). \quad (72)$$

In the most common case where the summation is limited to one term, that is to say when there is only one stationary point for all axis points, relation (61) is obvious.

We will not try to determine whether geometries exist which violate condition (61). We will use relation (72) to establish the coupling term between the axisymmetric motion of the structure and both internal and external fluids. The use of relation (58) implies that $U(y,k,\varepsilon)$ and $[P(y,k,\zeta,\varepsilon)]$

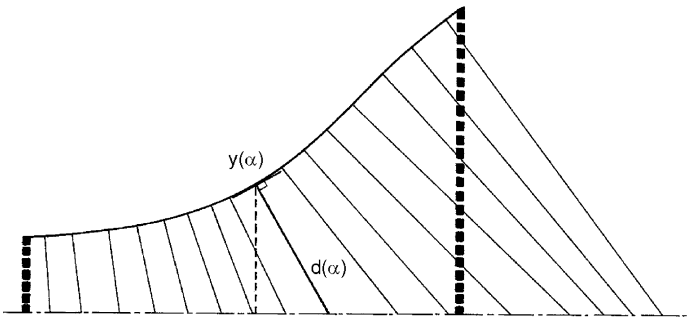

Fig. 4. Calculation of $d(\alpha)$ for a point $y(\alpha)$ of the meridian line.

evolve slowly inside the stationary lobe. We have shown in Ref. [30] that the results remain true when they evolve inside it.

The way to obtain these coupling terms is therefore as follows: a "stationary distance" is associated with each point on the meridian line. Fig. 4 shows that this distance corresponds to the length of the segment between the point and the intersection with the axis of the straight line carried by the normal n_y; it is this distance which local relation (72) deals with.

It is to be noted that a problem arises when the normal issued from a point of the surface leads to a point of the axis outside of the structure.

Actually, as already mentioned, the problem remains the same when it is extended by symmetry with respect to the rigid ends.

Thus, $d(\alpha)$ must be determined as if the ends did not exist, as shown in Fig. 4. This allows us to derive the third intermediary result.

Third intermediary result: Relation between the axisymmetric wall-pressure jump and the acceleration

$$[P(y(\alpha),k,\zeta,\varepsilon)]=\frac{\rho\omega^2\left(\frac{\mathrm{i}k/\zeta}{ik-(1/d(\alpha))}+\left(\mathrm{e}^{-d(\alpha)/\zeta}+\mathrm{e}^{-(k\varepsilon+(1/2\zeta))d(\alpha)}-1\right)^{-1}\right)}{\mathrm{i}k-(1/d(\alpha))-(\mathrm{i}k/\zeta)}(U(y(\alpha),k,\varepsilon),n_{y(\alpha)}). \tag{73}$$

The relation is strictly local.

5.1. Remark

Generally, $1/\zeta$ is much smaller than $k\varepsilon$, but both are very small in comparison with 1. Therefore, when k is sufficiently large in comparison with $1/d(\alpha)$, the coupling term simply results in the plane wave hypothesis:

$$[P(y(\alpha),k)]=\frac{\rho\omega^2}{\mathrm{i}k}(U(y(\alpha),k,\varepsilon),n_{y(\alpha)})=-\mathrm{i}\omega\rho c(U(y(\alpha),k,\varepsilon),n_{y(\alpha)}). \tag{74}$$

An easy asymptotic expansion in k, $1/\zeta$ and ε would give a more precise result, but this is not useful here.

6. Sructural modal expansion

$U(y,k,\varepsilon)$ is a linear combination of the axisymmetric modes of the structure in vacuo:

$$U(y,k,\varepsilon)=\sum_{m=-\infty}^{m=+\infty} b_m(k,\varepsilon)\phi_m(y), \tag{75}$$

where

$$\begin{aligned}&\sum_m b_m(k,\varepsilon)\left[-\omega^2 M-2\mathrm{i}\omega\varepsilon+K\right]\phi_m(y)=[P]n_y-E,\\&-\omega^2 M\phi_m+K\phi_m=0,\\&\int_S M\phi_m\phi_n\,\mathrm{d}\mu=\delta_m^n.\end{aligned} \tag{76}$$

The boundary conditions are to be given only on the edges of $S(S\cap(F_1\cup F_2))$ with the chosen shell equations.

Since the pressure jump due to the displacement of the structure $U(y,k,\varepsilon)$ alone is given by expression (73), the components of the wall displacement verify

$$b_m(k,\varepsilon)\left[\omega_m^2 M-2\mathrm{i}\varepsilon_m\omega_m\omega+Z_{mm}(k)-\omega^2\right]+\sum_{q\neq m} b_q(k,\varepsilon)Z_{mn}q(k)=-E_m, \tag{77}$$

assuming a diagonal form for the damping operator ε and calling E_m the components of the exterior field driving on the in vacuo structural modes ϕ_m and Z_{mq}, the coupling term between the structural modes ϕ_m and ϕ_q resulting from the fluid effect:

$$Z_{mq}(k)=\rho\omega^2\int_S \frac{\frac{\mathrm{i}k}{\zeta}+\left(\mathrm{e}^{-d(\alpha)/\zeta}+\mathrm{e}^{-(k\varepsilon+(1/2\zeta))d(\alpha)}-1\right)^{-1}}{\mathrm{i}k-\frac{1}{d(\alpha)}-\frac{\mathrm{i}k}{\zeta}}\left(\Phi_m(y),n_y\right)\left(\Phi_q(y),n_y\right)\mathrm{d}\mu(y). \tag{78}$$

The matrix, which connects the vector of components $b_m(k,\varepsilon)$ to the vector of components $E_m(k)$ when the system is truncated, is no longer diagonal. It is theoretically full and complex but remains symmetrical. Generally the crossing terms are weak. Their weakness can be appreciated by using the plane wave assumption and assuming that the mass operator M is diagonal with a constant value ρ_s and the normal component of the eigenvector ϕ_m predominant:

$$Z_{mq}(k)\cong\frac{\rho}{\rho_s}\frac{\omega^2}{\mathrm{i}k}\delta_m^q. \tag{79}$$

7. The complete method

We have gathered all the elements which enable us to propose a method for calculating the spectral density of the pressure at any point of the axis of an axisymmetric structure. We will now present this method step by step.

7.1. Excitation field on the blocked structure

The excitation field, that is to say the force field that would exist on the structure if it were perfectly rigid, may consist of mechanical forces, an acoustic pressure field diffracted by the blocked structure or a turbulent boundary layer, etc.

These fields need not be axisymmetric. Only their axisymmetric component has to be known:

$$E(y,k)=\frac{1}{2\pi}\int_{\theta=0}^{2\pi} e(y,\theta,k)\,\mathrm{d}\theta. \tag{80}$$

More precisely, only the power spectral density of that component needs to be known:

$$S_{EE}(y,y';\omega)=\lim_{T\to\infty}\frac{1}{T}\mathscr{E}[E(y;\omega;T)\overline{E(y;\omega;T)}], \tag{81}$$

where $-\mathscr{E}[\bullet]$ denotes expectation, $E(y;\omega;T)$ the time Fourier transform of $E(y;t)$ truncated at time T, and a bar over a symbol its conjugated value.

This power spectral density can be calculated or estimated. The cross-spectrum matrix can also be measured on a rigid model, which requires microphone crowns. It is essential to know these data for the following computation.

7.2. Axisymmetric in vacuo structural modes

This calculation can be performed with a finite element method because only axisymmetric modes are needed. Since their density tends to zero when the frequency tends to infinity—even if their number tends to infinity—they become sufficiently separated to be accessible through a finite element calculation.

To verify that the stationary phase method can be applied, the graphic method proposed in Ref. [30g] can be used as mentioned in Section 4.2.

7.3. Calculation of the fluid–structural mode coupling term

The general formulation of the problem has shown that this term comes from the linear dependence between the wall-pressure jump due to the wall displacement and the wall displacement itself.

We have shown that, for the particular case of axisymmetric in vacuo structural modes, the ratio between wall pressure and displacement was quite local and was easily calculated with formula (78), once parameter $d(\alpha)$ is known.

The coupling between the fluid and a structural mode consists of the effect of both external and internal fluids on the structure, supposedly vibrating on its in vacuo normal mode ϕ_m.

The determination of parameter $d(\alpha)$ was programmed for a truncated cone. This could have been easily generalized for any axisymmetric geometry.

Once this parameter $d(\alpha)$ is computed, the integration in formula (78) can be achieved for each in vacuo structural mode calculated in Section 7.2, which leads to the coupling term $Z_{mq}(k)$.

7.4. Structure displacement

The resolution of the complete fluid–structure coupling problem would have led to the following truncated system of equations [27,30]:

$$\begin{cases} \left(-\omega^2 M - 2\mathrm{i}\omega\xi + K\right) b_m = \sum_{n=-\infty}^{n=+\infty} \overline{C_{mn}} a_n - \left(e + p_n^e\right)_m, \\ \left(-\omega_m^2 - \frac{\mathrm{i}\omega}{\tau} - \omega^2\right) a_n = \rho c^2 \omega^2 \sum_{m=-\infty}^{m=+\infty} C_{mn} b_m, \end{cases} \tag{82}$$

calling a_n the component of the internal acoustic pressure on the modal basis $\{w_n\}$ (15), very close to the Neumann modal basis $\{u_n\}$, b_m the component of the structure displacement on its in vacuo modes basis $\{\phi_m\}$, C_{mn} the coupling factor between the acoustic mode w_n and the structural mode ϕ_m, and τ the reverberation time of the cavity. Furthermore, in this formulation, p^e would have been unknown and, in fact, would have depended linearly on the wall displacement U.

With the proposed method, the resulting truncated system is considerably simplified, since the acoustic problem is totally eliminated.

The remaining problem is reduced to a structural problem with a fluid–structure coupling term:

$$\left(-\omega_m^2 - 2\mathrm{i}\xi_m\omega_m\omega + Z_{mm}(k) - \omega^2\right) b_m(k,\varepsilon) + \sum_{q\neq m} Z_{mq}(k) b_q(k,\varepsilon) = -E_m(k). \tag{83}$$

Recalling that the axisymmetric structural mode density tends to zero, while the acoustic mode density grows to infinity, the time gain is considerable because now the matrix truncated system has a size equal to the number of calculated structural modes.

The acoustic problem would have required a much too high degree of freedom number; its resolution would have been numerically impossible, because of the frequency closeness of those acoustic modes.

Moreover, as Eq. (79) shows, in air, the coupling between different modes $(Z_{mq}(k), m\neq q)$ is generally much weaker than the diagonal term, which makes it possible to avoid a matrix inversion in the resolution of Eq. (83), by simply considering:

$$b_m(k,\varepsilon) \cong \frac{-E_m(k)}{-\omega_m^2 - 2\mathrm{i}\xi_m\omega_m\omega + Z_{mm}(k) - \omega^2}. \tag{84}$$

7.5. Final expression

An approximate transfer function $H^a(y,y';\omega,\varepsilon)$ between the axisymmetric components of the excitation and the normal displacement $\left(U(y,k,\varepsilon), n_y\right)$ is thus easily obtained with simplification (84):

$$H^a(y,y';\omega,\varepsilon) = \sum_{m=-\infty}^{m=+\infty} \frac{\left(\phi_m(y), n_y\right)\phi_m(y')}{\omega_m^2 - 2\mathrm{i}\xi_m\omega_m\omega + Z_{mm}(\omega/c) - \omega^2}. \tag{85}$$

If one does not want to use simplification (84), one can always invert the matrix system (83) to derive the exact transfer function between the axisymmetric components of the excitation $E(y',k)$

and those of the displacement $\left(U(y,k,\varepsilon),n_y\right)$:

$$H^a(y,y';\omega,\varepsilon)=\sum_{m=-\infty}^{m=+\infty} b_m\left(\frac{\omega}{c},\varepsilon\right)\left(\phi_m(y),n_y\right)\phi_m(y'). \tag{86}$$

One of these last two equations can be used to compute the internal pressure on the axis with formula (59). The integration could be performed with the stationary phase method through formula (58). However, this is not necessary. The stationary phase method has been used to derive theoretical results. To save time, the integration could be limited to the portion of the meridian line included in the lobe of the stationary phase, but it is simpler to integrate more roughly on the whole meridian line. Indeed, integration in Eq. (59) will be better performed that way. Details of the programming of all these points are given in Ref. [30, French version only].

8. Application to a truncated cone

8.1. Description of the experiment

We have applied this method to a 2.50-m-long truncated cone, made of a 1-cm-thick composite material, closed by two rigid lead plates, 0.182 m in diameter at the front and 0.693 m in diameter at the back. It was suspended at the front and the back by slings. The experiment was conducted inside a reverberating room (3.70 m × 3.70 m × 2.10 m).

The characteristics adopted for calculating the structure are described in detail in Ref. [30i], as well as the approximations for determining the pressure inside the reverberating room [30j].

Only the ten first axisymmetric modes of the structure have been computed. The complete calculation has been performed with the same 7% damping factor for each structural mode. The wall was covered with a 2500 $\mathrm{kg\,m^{-2}\,s^{-1}}$ acoustic impedance cork, equivalent to a 30 ms cavity reverberation time.

For the sake of simplicity, expression (82) has been used instead of Eq. (83). The power spectral density of the pressure field inside the reverberating room, fed with white noise through loud speakers in the 0–2500 Hz range, is shown in Fig. 5.

The parallel of latitude on which the wall acceleration summation has been calculated and the four axis points on which the pressure has been computed are indicated in Fig. 6.

The acoustic driving field is not precisely known, nor are the mechanical characteristics of the structure, especially its resonance frequencies. The aim of this experiment is only to give a clear understanding of the tractability of the proposed method.

8.2. Comparison of the measured and computed results

The results will be given in linear scale, and thus not converted into decibel, since we are only interested in the level at the resonance peaks.

Fig. 7 shows the comparison between the measured and computed wall acceleration summations. The calculation has been performed with and without fluid–structure coupling terms.

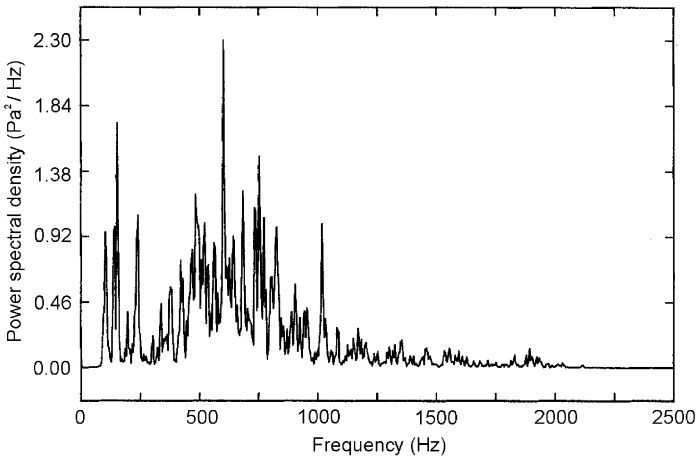

Fig. 5. Pressure field in the reverberant room.

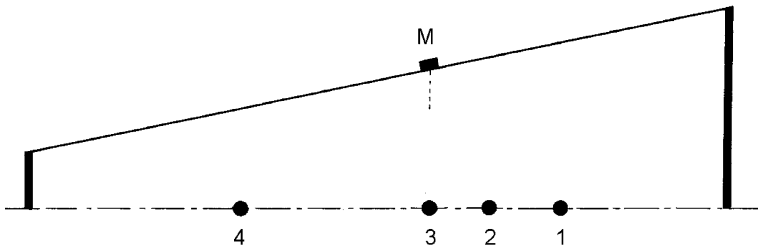

Fig. 6. Summation of the wall acceleration calculation and comparison with measurement: parallel of latitude (M). Pressure calculation on the axis and measurement points 1, 2, 3, and 4.

The pressure power spectral densities measured and computed at location points 1, 2, 3, and 4 of Fig. 6 are compared in Fig. 8.

8.3. Analysis of results

Recalling that the aim of this experiment is only to show the tractability of the proposed method and considering the imprecise knowledge of the acoustic driving field and the mechanical characteristics of the structure, the agreement between the measurements and calculations is not perfect (poor superposition of the power spectral densities), all the more so since the computation is performed in a frequency domain in which the performance of the method is not best (the higher the frequency, the better suited the method).

However, the levels of the computed power spectral densities are satisfactory, which reflects a good representation of the physical reality. The computation of 100 structural modes (with one thousand degrees of freedom instead of one hundred on the meridian line) would have greatly improved the power spectral densities and largely increased the analysed bandwidth.

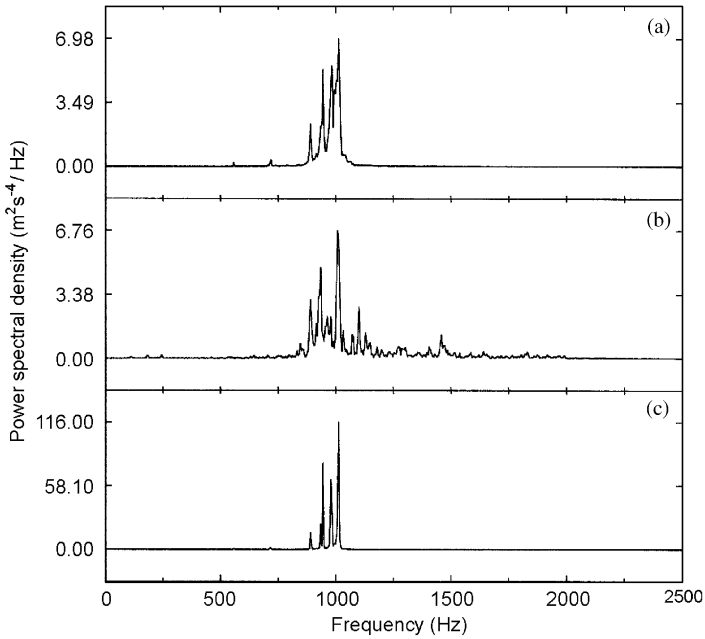

Fig. 7. Summation of accelerations on the parallel of latitude M: (a) calculated with coupling, (b) measured and (c) calculated without coupling.

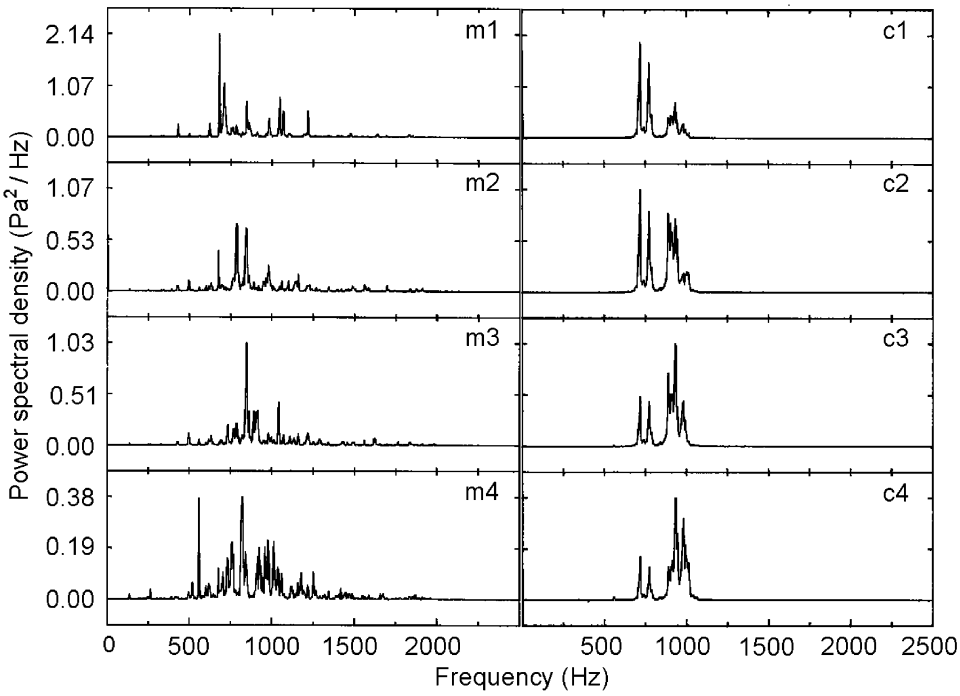

Fig. 8. Comparison of the measured (m) and calculated (c) pressure at points 1, 2, 3, and 4.

9. Conclusion

We propose an easily programmable method for computing the acoustic pressure inside an axisymmetric enclosure, since only the in vacuo structure axisymmetric modes are needed.

It is suitable for most aeronautical airborne structures, not only above the coincidence frequency but at any frequency, because curvature has the determining effect of increasing the lowest resonance frequency of the axisymmetric structural modes.

It gives the fluid–structure coupling terms without resolution of the Helmholtz equation.

The final result is the power spectral density of the pressure on the axis when the structure is excited by any force field, for a wide frequency band, and not only for a single frequency.

An experiment, carried out in a reverberating room, shows its tractability and gives satisfactory results considering the lack of knowledge about the structure and the room pressure.

The use of the stationary phase method for points outside the axis and non-axisymmetric cavities would probably lead to the generalization of intermediary results 2 and 3, and thus of the complete method for any point inside any kind of structure, but to a lesser degree with regard to a higher frequency domain.

References

[1] E.H. Dowell, Master plan for prediction of vehicle interior noise, *American Institute of Aeronautics and Astronautics Journal* 18 (1980) 353–366.
[2] P.W. Smith, Sound transmission through thin cylindrical shells, *Journal of the Acoustical Society of America* 29 (1957) 721–729.
[3] L.R. Koval, The effect of airflow panel curvature and internal pressurization on field incidence transmission loss, *Journal of the Acoustical Society of America* 59 (1976) 1379–1385.
[4] L.R. Koval, On sound transmission into a thin cylindrical shell under flight conditions, *Journal of Sound and Vibration* 48 (1976) 265–275.
[5] L.R. Koval, Effect of stiffening on sound transmission into a cylindrical shell in flight, *American Institute of Aeronautics and Astronautics Journal* 15 (1977) 899–900.
[6] L.R. Koval, Effect of longitudinal stiffeners on sound transmission into a thin cylindrical shell, *Journal of Aircraft* 15 (1978) 816–821.
[7] L.R. Koval, On sound transmission into a heavily damped cylinder, *Journal of Sound and Vibration* 57 (1978) 155–156.
[8] L.R. Koval, Effects of cavity resonances on sound transmission into a cylindrical shell, *Journal of Sound and Vibration* 59 (1978) 23–33.
[9] L.R. Koval, On sound transmission into an orthotropic shell, *Journal of Sound and Vibration* 63 (1979) 51–59.
[10] L.R. Koval, Sound transmission into a laminated composite cylindrical shell, *Journal of Sound and Vibration* 71 (1980) 523–530.
[11] L.R. Koval, On sound transmission into a stiffened cylindrical shell with rings and stringers treated as discrete elements, *Journal of Sound and Vibration* 71 (1980) 511–521.
[12] J.A. Cockburn, A.C. Jolly, Structural acoustic response, noise transmission losses and interior noise levels of an aircraft fuselage excited by random pressure fields, *US Air Force Flight Dynamics Laboratory Report*, 68-2, 1968.
[13] L.D. Pope, On the transmission of sound through finite closed shells: statistical energy analysis, modal coupling and non-resonant transmission, *Journal of the Acoustical Society of America* 50 (1971) 1004–1018.
[14] L.D. Pope, J.F. Wilby, Band-limited power flow into enclosures, *Journal of the Acoustical Society of America* 62 (1977) 906–911.
[15] L.D. Pope, J.F. Wilby, Space shuttle payload bay acoustics prediction study, vol. II: analytical model, *NASA CAR* 159.956, 1980.

[16] L.D. Pope, J.F. Wilby, Band-limited power flow into enclosures, *Journal of the Acoustical Society of America* 67 (1980) 823–826.
[17] L.D. Pope, C.M. Willis, W.H. Hayes, Propeller aircraft interior noise model—part II: scale-model and flight-test comparisons, *Journal of Sound and Vibration* 118 (1987) 469–494.
[18] L.D. Pope, E.G. Wilby, J.F. Wilby, Propeller aircraft interior noise model—part I: analytical model, *Journal of Sound and Vibration* 118 (1987) 449–468.
[19] J.F. Unruh, Finite element sub volume technique for structural-borne interior noise prediction, *Journal of Aircraft* 17 (1980) 434–441.
[20] R.H. Lyon, *Statistical Energy Analysis of Dynamical Systems: Theory and Applications*, Massachusetts Institute of Technology Press, Cambridge, 1975.
[21] R. Vaicatis, Noise transmission by viscoelastic sandwich panels, *NASA TN* 0-8516, 1977.
[22] R. Vaicaitis, M. Slazak, H.T. Chang, Noise transmission—turboprop problem, *American Institute of Aeronautics and Astronautics Paper* 79-0645, 1979.
[23] R. Vaicaitis, M. Slazak, Noise transmission through stiffened panels, *Journal of Sound and Vibration* 70 (1980) 413–426.
[24] H.T. Chang, R. Vaicaitis, Noise transmission into semi-cylindrical enclosures through discretely stiffened curved panels, *Journal of Sound and Vibration* 85 (1982) 71–83.
[25] Y.K. Lin, *Probabilistic Theory of Dynamical Systems: Theory and Applications*, Massachusetts Institute of Technology Press, Cambridge, 1967.
[26] Y.K. Lin, B.K. Donaldson, A brief survey of transfer matrix techniques with special references to the analysis of aircraft panels, *Journal of Sound and Vibration* 10 (1969) 103–143.
[27] E.H. Dowell, G.F. Gorman III, D.A. Smith, Acousto-elasticity: general theory, acoustic natural modes and forced response to sinusoidal excitation, including comparisons with experiments, *Journal of Sound and Vibration* 52 (1977) 519–542.
[28] L. Meirovitch, A new method of solution of the eigenvalue problem for gyroscopic systems, *American Institute of Aeronautics and Astronautics Journal* 12 (1974) 1337–1342.
[29] A.D. Pierce, *Acoustics: An Introduction to its Physical Principles and Applications*, Mac Graw-Hill Book Company, New-York, 1981.
[30] D. Brenot, Transmission of sound inside an axisymmetric structure, Ph. D. Thesis, Translation in English of Transmission du son à l'intérieur d'une structure axisymétrique: Thèse de Doctorat d'Etat. Publication ONERA P 1987-1 by the European Space Agency: ESA-TT-1218, NP. 248 (N91-30908/8/XAD (NTIS));
[a] See pp. 27–33 (F) or pp. 40–46 (E);
[b] See pp. 21–23 (F) or pp. 33–35 (E);
[c] See pp. 54–57 (F) or pp. 70–74 (E);
[d] See pp. 122–123 (F) or pp. 149–150 (E);
[e] See pp. 78–90 (F) or pp. 98–112 (E);
[f] See pp. 88–90 (F) or pp. 109–112 (E) 30e;
[g] See pp. 113–119, 152–163 (F) or pp. 138–146, 184–188 (E);
[h] See pp. 23–26 (F) or pp. 35–39 (E);
[i] See pp. 144–145, 193–197 (F), or pp. 174–176 (E);
[j] See pp. 150–151 (F) or pp. 181–183 (E).
[31] P.M. Morse, H. Feshbach, *Methods of theoretical physics*, vol. 1, Mac Graw-Hill Book Company, New-York, 1953.
[32] A. Erdelyi, *Asymptotic Expansions*, Dover Publications Inc., 1956.
[33] J.E. Manning, G. Maidanik, Radiation properties of cylindrical shells, *Journal of Sound and Vibration* 36 (1964) 1691–1698.